Mineralogical Magazine, June 2000, Vol. 64(3), pp. 447–457

Total scattering studies of silica polymorphs: similarities in glass and disordered crystalline local structure

D. A. KEEN[1,*] AND M. T. DOVE[2]

[1] ISIS Facility, Rutherford Appleton Laboratory, Chilton, Didcot, Oxfordshire OX11 0QX, UK
[2] Department of Earth Sciences, Cambridge University, Downing Street, Cambridge CB2 3EQ, UK

ABSTRACT

The structure of amorphous silica has frequently been compared with its crystalline counterparts in an attempt to understand the glass structure beyond short-range correlations. This paper presents results from neutron total scattering measurements of several polymorphs of silica and shows how these can be used to make a direct, quantitative comparison of amorphous and crystalline forms. It is found that the glass is similar to HP-tridymite and β-cristobalite, both dynamically-disordered crystalline phases of silica, but only out to distances ~7.5 Å, beyond which the structures diverge. This is too small to validate a microcrystallite theory of glass structure. It is the average 180° Si–O–Si linkage in these two crystalline phases which gives them the flexibility for their instantaneous disordered structure to resemble the quenched (static) glass structure.

KEYWORDS: total scattering, silica polymorphs, amorphous silica, glass.

Introduction

AMORPHOUS silica is considered the archetypal network glass consisting of a simple continuous random network of corner-linked SiO_4 tetrahedra (Zachariasen, 1932). The structure has been much studied, modelled and debated (Wright, 1994). Despite this, the specifics of the longer-range structure, i.e. structure beyond nearest and next-nearest neighbours, have not been determined unambiguously, although several models exist including the interstitial void model (Elliott, 1995) and the quasi-Bragg plane interpretation (Gaskell and Wallis, 1996). This latter model is motivated by the similarity in the position of the glass so-called first sharp diffraction peak (FSDP) and the first Bragg peak in β-cristobalite, the crystalline phase of silica which is considered most similar to the glass. It is this comparison which this paper sets out to quantify, not by importing the language of crystal structure characterization into the glass structural description (as in the quasi-Bragg plane interpretation) but rather by using total scattering analysis of the crystalline structures (methods more usually applied to glasses) to quantify the local structural disorder in the crystal and thus allowing direct comparison of glass and crystal local structures.

When considering total scattering measurements of crystalline materials it is important to make the distinction between the 'average' and 'instantaneous' structure. The structural description which is obtained from interpretation of Bragg scattering (elastic scattering) is an average structure, or more precisely it is a time-average structure since elastic scattering gives the correlation between an atom and itself at different times. The characterization of this scattering in terms of a model which is a periodic repetition of a unit cell means that (for a crystal) it can also be considered as a spatial average of the structure. In contrast an instantaneous structure is obtained from total scattering (Bragg and diffuse, elastic and inelastic scattering) giving information about correlations between different atoms at an instant of time, a 'snap-shot' of the structure. For a regular structure these two descriptions may be very similar, but when the structure is very

* E-mail: d.a.keen@rl.ac.uk

disordered, they may be very different since atoms may, at an instant of time, be very far from their average positions.

Neutron total scattering measurements from various crystalline phases of silica are shown in Fig. 1 and compared with the total scattering from silica glass (Grimley *et al.*, 1990). The high-Q scattering (Fig. 1*c*) is very similar in all cases, reflecting the local corner-sharing SiO_4 tetrahedral environment common to all phases shown. At low-Q the high-temperature crystalline phases still show diffuse scattering (Fig. 1*b*), although at a much reduced intensity to that seen in the glass. Figure 1*a* shows an enlarged Q-region around the FSDP showing the similarity in position of the first Bragg peaks in cristobalite and HP-tridymite and the FSDP of the glass.

Modelling the total scattering data

The approach used here to model the total scattering data is based on the reverse Monte Carlo (RMC) modelling method (Keen and McGreevy, 1990), but adapted to maintain the regular SiO_4 tetrahedra and the structures' connectivity. This is achieved by using the following constraints:

$$\chi^2_{\text{constraints}} = \Sigma(r_{\text{Si-O}} - R_{\text{Si-O}})^2/\sigma_r + \Sigma(\theta_{\text{O-Si-O}} - \Theta_{\text{O-Si-O}})^2/\sigma_\theta \quad (1)$$

where the first term is the squared difference between the actual Si–O bond length $r_{\text{Si-O}}$ and the ideal value $R_{\text{Si-O}}$ summed over all Si–O bonds in the structure and the second term is the squared difference between the actual intra-tetrahedral bond angles $\theta_{\text{Si-O-Si}}$ and the ideal value of 109.47°, summed over all such bond angles. Implicit in these definitions is the retention of the starting model's connectivity and in practise they are calculated using a list of nearest neighbour atoms. Having created a suitable starting model which satisfies these constraints (see below), the model is adjusted so as to fit the total scattering using the usual (constrained) RMC χ^2:

$$\chi^2 = \Sigma(F_{\text{calc}}(Q_i) - F_{\text{expt}}(Q_i))^2/\sigma(Q_i)^2 + \chi^2_{\text{constraints}} \quad (2)$$

summing over all the Q points in $F(Q)$ and maintaining the above constraints. The value of $\sigma(Q_i)$ is slowly reduced with respect to σ_r and σ_θ until a good fit to the total scattering data has been obtained. More details of this method may be obtained in Keen (1998).

Glass starting model

The method of producing the silica glass starting model has been described in Keen (1997) and will only be outlined briefly here. Silicon and oxygen atoms in the correct proportion were placed in a cubic box of a size to give the correct density. These atoms were moved randomly under periodic boundary conditions. When two unlike atoms which are not already fully co-ordinated approach each other within a certain distance they 'bond'. Once atoms are bonded they continue to move, but by smaller amounts, and the constraints in equation 1 (as well as a similar, but weaker, angle constraint on the Si–O–Si linkage to restrain it to 143° and thus reduce the likelihood of forming three-membered rings) are imposed on them to regularize the network structure. This procedure is continued until no further atoms may be added. At this point, some of the bonds are allowed to break and atoms swap to change the connectivity but not the overall co-ordination. This 3000-atom model, when no further improvement to the overall bonding could be achieved, had an average of 3.9 O atoms around each silicon and 1.95 Si atoms around each oxygen and regular SiO_4 tetrahedra. The agreement with available structure factor data was very good, except that it did not fit the FSDP well (Keen, 1997).

Crystal starting models

Rietveld refinement (see Young, 1995, for example) of the powder diffraction patterns provided the basis for the starting crystalline models. Figure 2 shows two possible refined average structural models for β-cristobalite, both in space group $Fd\bar{3}m$, and following the work of (Schmahl *et al.*, 1992). Figure 2*a* shows an average structure where the O atoms sit on 16*c* (000) sites exactly midway between neighbouring Si atoms which are on 8*a* (1/8,1/8,1/8) sites. This gives an unphysical 180° Si–O–Si linkage, a Si–O bond length which is too short, and although it is a model which agrees well with the data, it does not characterize the local structure accurately. Indeed the refined anisotropic thermal parameters are such as to elongate the O density in the directions perpendicular to the Si–Si direction suggestive of a preference for a more acute Si–O–Si linkage. A more accurate characterization of the O atom distribution can be seen in Fig. 2*b*, where the oxygen 16*c* positions have been split into 96*h* (0*xx*) sites, each 1/6$^{\text{th}}$ occupied, with $x \approx 0.05$. This gives a better agreement with the data, a more physical

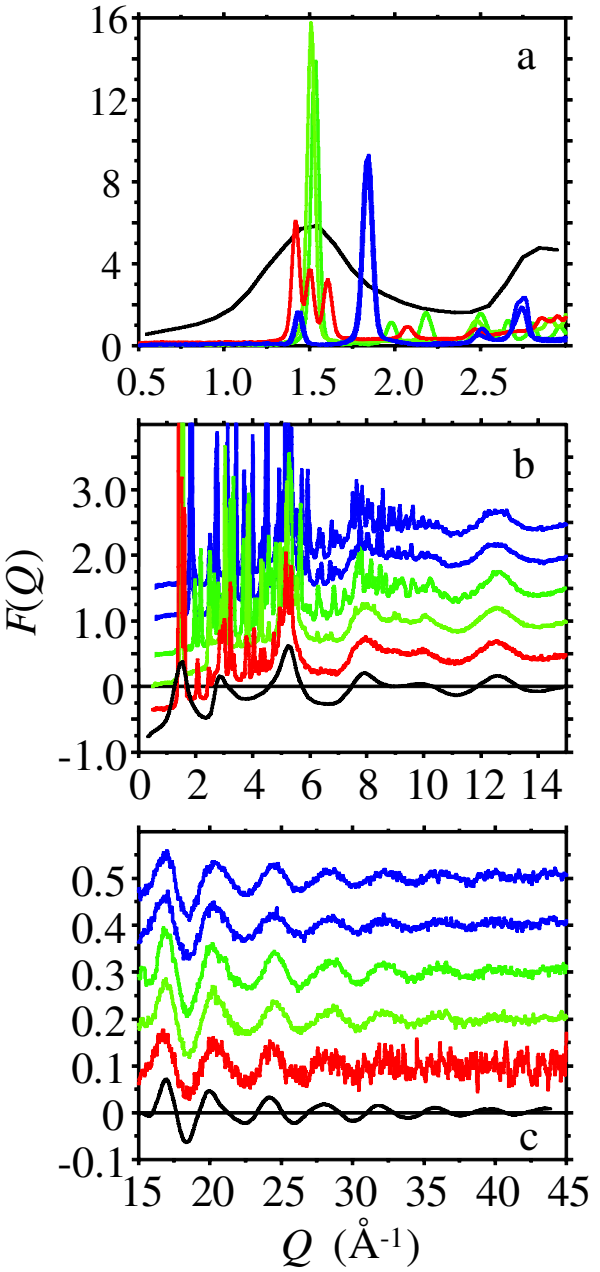

FIG. 1. Total scattering structure factors, $F(Q)$, from various silica polymorphs: (*a*) in the region of the glass FSDP (the glass $F(Q)$ has been scaled for clarity). The two strong peaks at ~1.5 $Å^{-1}$ are from α- and β-cristobalite, the set of three peaks in the same region come from HP-tridymite and the strong peaks at ~1.8 $Å^{-1}$ are from α- and β-quartz (together with a weak peak at ~1.4 $Å^{-1}$). (*b*) and (*c*) show normalized $F(Q)$ at low- and high-Q respectively. The data are from silica glass at room temperature (Grimley *et al*., 1990), HP-tridymite at 550°C, β-cristobalite at 300°C, α-cristobalite at 200°C, β-quartz at 620°C and α-quartz at 500°C with each successive plot offset vertically by 0.5 and 0.1 in (*b*) and (*c*) respectively.

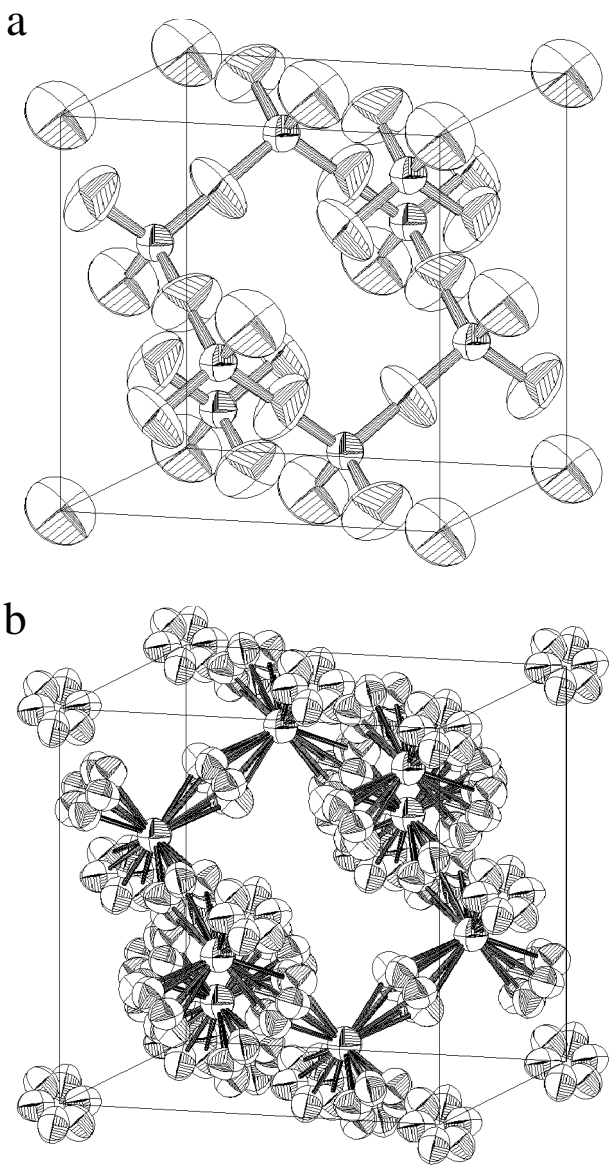

FIG. 2. Two average structural models for β-cristobalite, from Rietveld refinement of the Bragg scattering component of neutron total scattering data measured at 300°C. (*a*) with O atoms on 16*c* sites and; (*b*) split equally between 96*h* sites (in space group $Fd\bar{3}m$, see text for details).

Si–O–Si angle and the density is seen to have a minimum at the 16*c* position and resulted in suggestions of a domain-based structure of β-cristobalite (Hatch and Ghose, 1991). However as Table 1 shows, this model is still not correctly reproducing the temperature dependence of the structure. The Si–O bond length, although of a physically sensible size, apparently contracts with increasing temperature and the Si–O–Si linkage angle becomes less acute. In contrast, the values of Si–O bond length and Si–O–Si angle determined from the radial distribution function (the Fourier transform of the total scattering structure factor) behave physically, although the value of the

TABLE 1. Tabulated values of the intra-tetrahedral Si–O bond length and inter-tetrahedral Si–O–Si linkage angle for cristobalite. Columns 2 and 3 come from Rietveld refinement of the Bragg scattering in space group $Fd\bar{3}m$ with the O atoms on 16*c* sites; columns 4 and 5 have the oxygens split between 96*h* sites and the values for the α-phase are from a refinement in space group $P4_12_12$. The values in the final two columns are obtained from the positions of the first (Si–O) and third (Si–Si) lowest-*r* peaks in $G(r)$ or (values in parentheses) the Si–O peak position in $G(r)$ and the Si–Si distance obtained from Rietveld refinement.

T (°C) (Phase)	16*c* (000) Si–O (Å)	Sites Si–O–Si(°)	96*h* (0*x*-*x*) Si–O (Å)	Sites Si–O–Si(°)	*G*(*r*) Si–O (Å)	Si–O–Si(°)
200(α)	(1.597	148.9)			1.606	147 (146.7)
300(β)	1.5443	180	1.6124	146.6	1.606	151 (148.1)
425(β)	1.5455	180	1.6104	147.4	1.608	150 (147.9)
500(β)	1.5464	180	1.6098	147.7	1.609	149 (147.9)
675(β)	1.5470	180	1.6073	148.5	1.611	150 (147.6)

Si–O–Si angle is not well determined because of the Si–Si peak in $G(r)$ is very weak. This angle is seen to be approximately constant with temperature when determined from the Si–O peak in $G(r)$ and the Si–Si distance obtained from Rietveld refinement which is reliable since the Si atoms do not disorder anisotropically. It should be pointed out that methods exist to correct the average structure to account for increased rigid body motion and thus extract reliable bond lengths and angles (see Downs *et al*., 1992, for example) – the advantage of using $G(r)$ is that the bond lengths may be obtained directly in a model independent manner.

The following method was chosen to create the initial structural model for RMC refinement of the crystalline systems. The average structure, from Rietveld refinement of a model which did not include any split-site occupancy, was used to construct a configuration of ~24,000 atoms, sitting on their ideal sites, with an integer number of unit cells in each direction. This model was then relaxed, by moving the atoms small distances and following the constraints in equation 1, with the Si–O distance measured from the first peak in $G(r)$. These starting models therefore reproduce the short-range order and are consistent with the long-range periodicity, but do not necessarily reproduce the effect of thermal vibration correctly.

Results and discussion

Good agreement with the data was obtained in all cases (e.g. Fig. 3 or Keen, 1997), without distorting the SiO_4 tetrahedra significantly or changing the starting connectivity. The final glass configuration now also reproduces the FSDP and the crystalline configurations produced diffuse scattering in certain reciprocal lattice planes which was consistent with published electron diffraction results (Keen, 1998). Therefore these configurations are good representations of the instantaneous structure. Figure 4 shows a section perpendicular to the *c*-axis of one configuration of HP-tridymite. The layers have been buckled and distorted significantly away from their ideal arrangement, but the crystalline order is retained. Figure 5 shows the partial and total radial distribution functions from the refined models of various phases of silica. On first inspection all the $T(r)$ (which is proportional to $rG(r)$) look qualitatively similar, varying only by the amount the peaks are damped at higher *r*-values. Closer inspection shows that there are also more important differences in the peak positions. β-cristobalite and α-cristobalite have peaks significantly out of phase by $r >$ ~6 Å. This means that models which have been proposed (Hatch and Ghose, 1991) where β-cristobalite is composed of an average of α-cristobalite domains cannot be correct. The differences between α- and β-quartz are less pronounced, but they are still significant enough to come to a similar conclusion (for example the peak in the β-quartz $T(r)$ at ~6.5 Å is split into a double peak in α-quartz). However, perhaps the most striking result which may be seen in Fig. 5 is the similarity in $T(r)$, $g_{Si-O}(r)$ and $g_{O-O}(r)$ of silica glass and β-cristobalite and HP-tridymite which have

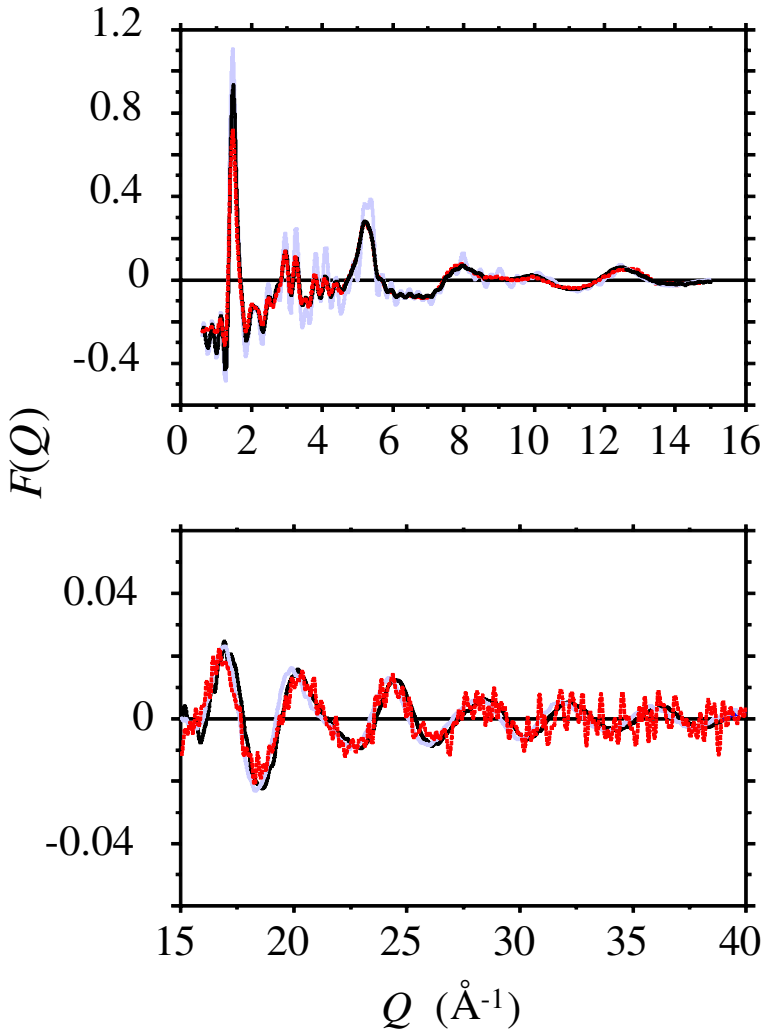

FIG. 3. Comparison of the convoluted $F(Q)$ data from HP-tridymite at 550°C (dotted line) with the structure factor calculated from the initial model (grey line) and from the final RMC refined model (full line). (The $F(Q)$ data have been convoluted with the Fourier transform of a box function of the size of half the shortest length of the RMC configuration to make direct comparison between experimental and calculated $F(Q)$ possible (Keen, 1998)).

peaks in phase up to at least 10 Å with similar relative intensities. In order to make a more formal comparison, the following function may be considered:

$$g_{\text{glass}}(r) = \exp(-r/\xi)g_{\text{crystal}}(r) + [1 - \exp(-r/\xi)]g_{\text{random}}(r) = \exp(-r/\xi)[g_{\text{crystal}}(r) - 1] + 1 \quad (3)$$

In other words, the glass correlation functions can be considered as a combination of crystalline and random correlation functions, controlled by a correlation length ξ. Below ξ the crystalline $g(r)$ dominates and above ξ random behaviour prevails. The best fit to the amorphous $g_{\text{Si-O}}(r)$ is obtained from HP-tridymite with a value of $\xi \approx 7.5$ Å. This also gives a reasonable agreement to $g_{\text{O-O}}(r)$ and the functions from β-cristobalite yield similar correlation lengths. Hence the similarities between glass and these crystal phases only extend over this length scale. This

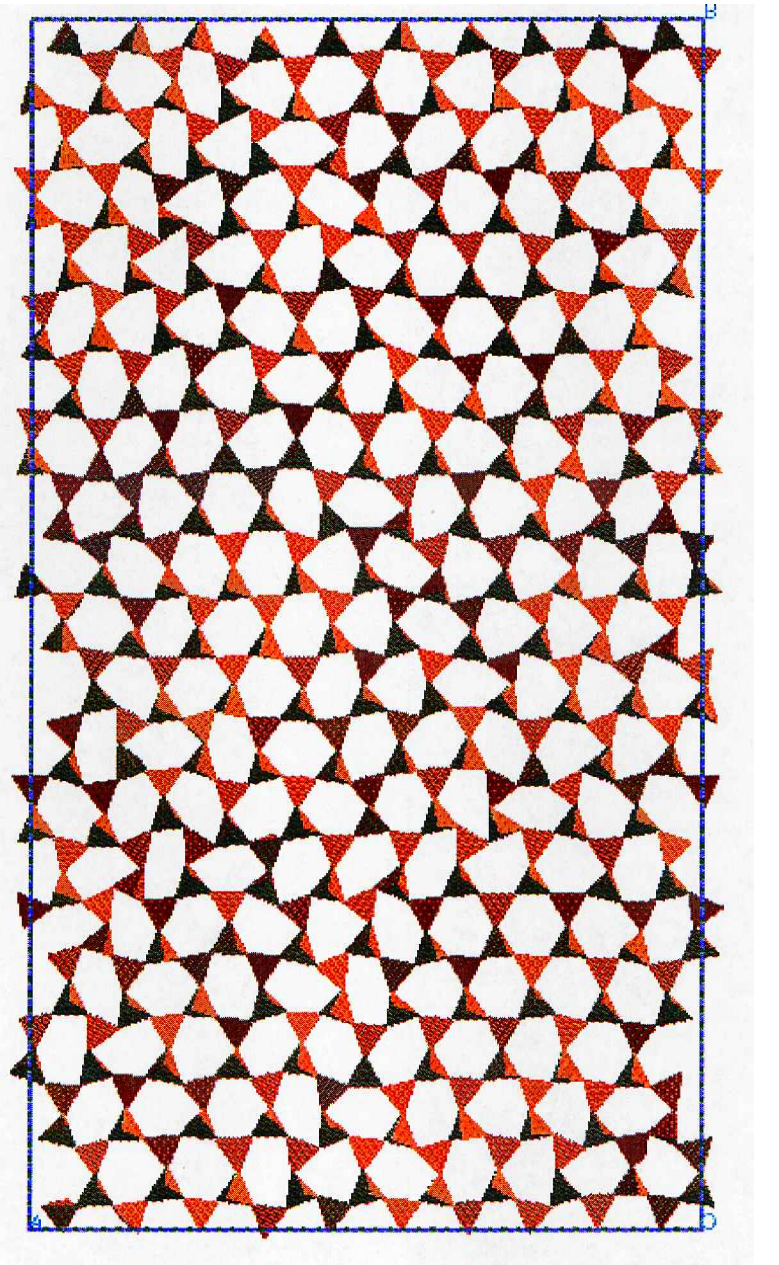

FIG. 4. A section perpendicular to the *c*-axis of a RMC-refined configuration of HP-tridymite at 550°C, showing that, despite the tetrahedral buckling which distorts the local environment, the crystalline network is retained. Each small tetrahedron shown corresponds to a corner-sharing SiO_4 unit.

is too short a distance to admit an interpretation along the lines of the existence of microcrystals of cristobalite or tridymite within the glass structure and one cannot even say that the structures are identical over these distances. Instead, these results indicate that there are regions in the glass of size ~ξ that have the same structural elements as in the crystal and beyond this distance

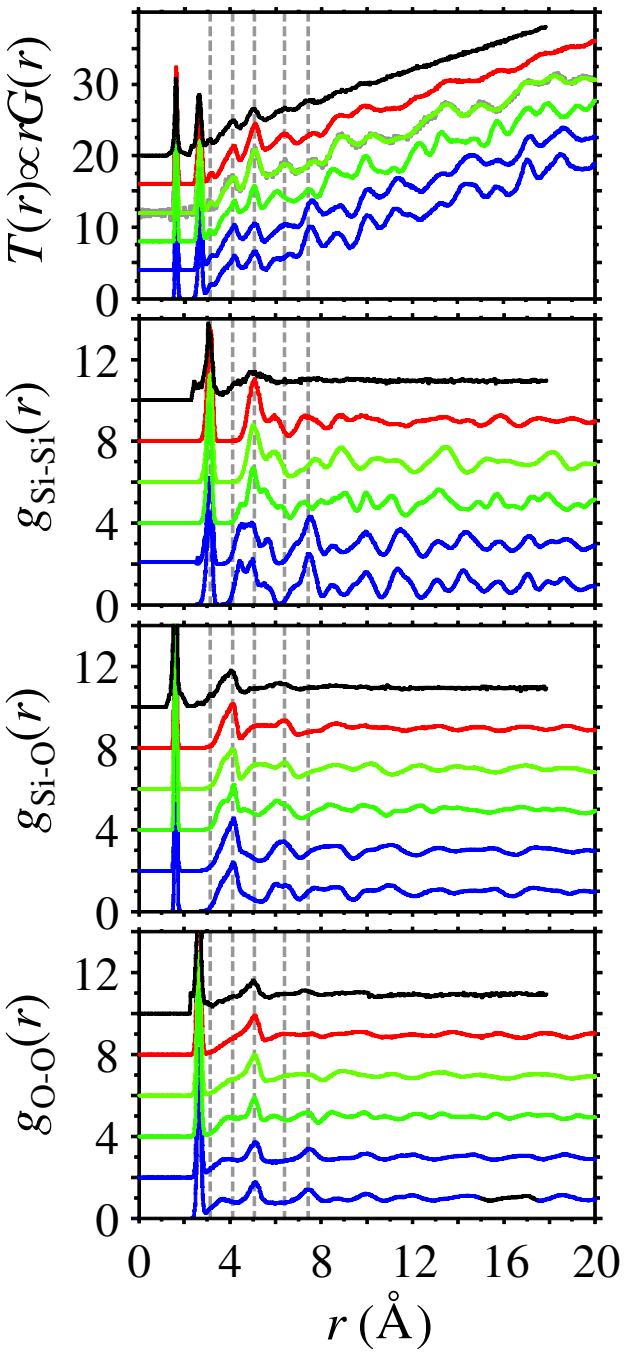

FIG. 5. Radial distribution functions from the RMC-refined models of various phases of silica at different temperatures, each successive plot is offset vertically for clarity. They are: α-quartz at 500°C (lowest plots), β-quartz at 620°C, α-cristobalite at 200°C, β-cristobalite at 300°C, HP-tridymite at 550°C and silica glass at room temperature (uppermost plots). The $T(r)$ for β-cristobalite is superposed on the $T(r)$ obtained from directly transforming $F(Q)$. Vertical dashed lines mark the positions of the most significant inter-tetrahedral peaks in the silica glass $T(r)$.

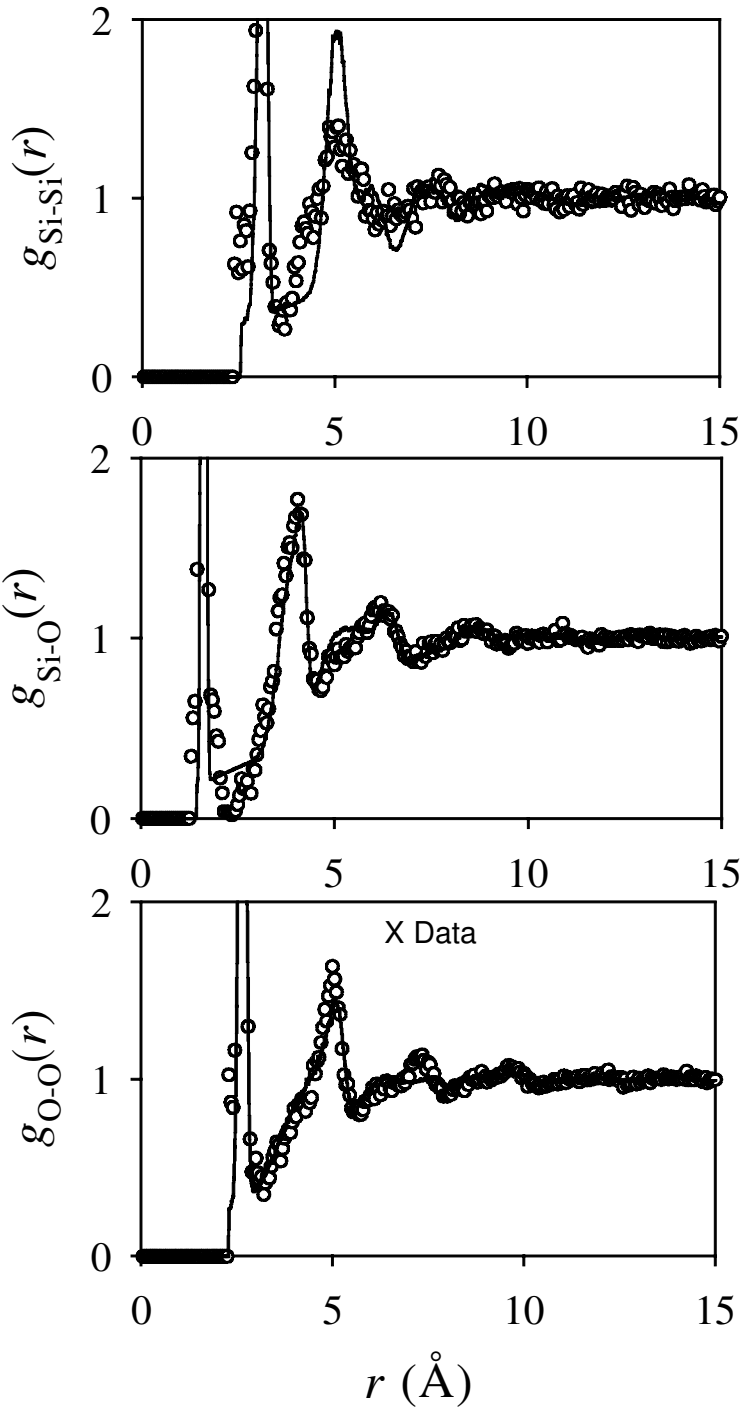

FIG. 6. Partial radial distribution functions from RMC refinement of silica glass (circles) plotted against a best-fit of equation 3 using the partial $g(r)$ of HP-tridymite and a correlation length of 7.5 Å (line).

the structures diverge. The reason that the structures diverge at longer distances is seen in $g_{Si-Si}(r)$ which remains highly oscillatory for the crystal structures but almost flat in the glass (Fig. 5). The Si–Si network forms the 'backbone' of the silica structures and determines the different symmetries of the different structures.

Figure 7 shows the local bond-angle distributions plotted against cosθ. The uppermost panel shows the regular nature of the SiO_4 tetrahedra in all cases. The middle panel shows how the O atoms disorder between neighbouring Si atoms. The plotted function is equivalent to the more usual bond-angle function (plotted against θ) divided by the solid angle which goes as sinθ. This has the effect of overemphasising the probability of finding 180° Si–O–Si linkages. Even despite this, all distributions peak at a value of $\cos\theta \neq -1$, with a width which is dependent on the amount of O disorder permitted by the structure. The narrowest distributions are from α-cristobalite and α-quartz and the broadest from HP-tridymite and silica glass. The amount of O disorder, or the amount by which the SiO_4 may rotate about their centres of mass, is determined by the Si network. The lowermost panel of Fig. 7 shows the Si–Si–Si bond angle distribution. β-cristobalite and HP-tridymite have one peak at the tetrahedral angle whereas all the other crystalline phases possess peaks at other angles. The distribution for the glass configuration is very broad, but also peaked at the tetrahedral angle. Structures with tetrahedral Si–Si–Si angles allow the greatest amount of SiO_4 rotation and this is why the oxygen disorder is greatest in these structures. Non-tetrahedral Si–Si–Si angles will tend to pin the SiO_4 tetrahedra into specific conformations. The glass structure is very disordered, but also has this characteristic Si–Si–Si tetrahedral angle. This is why the instantaneous local structures of dynamically-disordered β-cristobalite and HP-tridymite resemble that of the static disordered glass structure. The model produced from a total scattering measurement is a picture of the structure as if all the atoms undergoing dynamic processes have been frozen instantaneously – exactly what happens during the physical process of glass formation. However, although the disorder is similar between these three structures at the local level, the structures remain distinct because the Si 'backbone' is different in each structure.

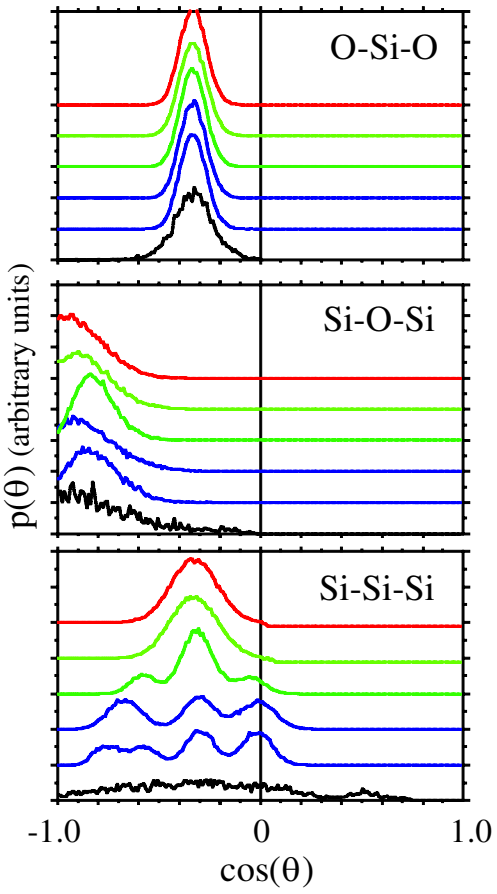

FIG. 7. Bond angle distribution functions from RMC-refined models of various phases of silica with each successive plot offset vertically for clarity. They are: silica glass at room temperature (lowest plots), α-quartz at 500°C, β-quartz at 620°C, α-cristobalite at 200°C, β-cristobalite at 300°C and HP-tridymite at 550°C (uppermost plots).

Conclusion

This paper has shown how it is possible to model total scattering data to produce local structural models of glass and crystalline systems which can be compared directly and self-consistently. The results from the various polymorphs of silica which have been studied show that β-cristobalite and HP-tridymite, the two stable highest temperature forms of ambient pressure crystalline silica, show very similar local disorder to that of the glass. These three structures are similar over distances of ~7.5 Å, beyond which the structures

diverge because of the distinct Si structural 'backbone' of each structure. They are similar over short distances because they all show tetrahedral Si–Si–Si angles which allow the maximum amount of SiO_4 rotation, a process which is dynamic in β-cristobalite and HP-tridymite and static in the glass. The other crystalline phases are distinct from the glass in relation to all but the nearest neighbour distances because non-tetrahedral Si–Si–Si angles constrain the SiO_4 tetrahedra rotation more severely.

References

Downs, R.T., Gibbs, G.V., Bartelmehs, K.L. and Boisen, M.B. (1992) Variations of bond lengths and volumes of silicate tetrahedra with temperature. *Amer. Mineral.*, **77**, 751–7.

Elliott, S.R. (1995) Second sharp diffraction peak in the structure of binary covalent network glasses. *Phys. Rev. B*, **51**, 8599–601.

Gaskell, P.H. and Wallis, D.J. (1996) Medium-range order in silica, the canonical network glass. *Phys. Rev. Lett.*, **76**, 66–9.

Grimley, D.I., Wright, A.C. and Sinclair, R.N. (1990) Neutron scattering from vitreous silica IV. Time-of-flight diffraction. *J. Non-Cryst. Sol.*, **119**, 49–64.

Hatch, D.M. and Ghose, S. (1991) The α-β phase transition in cristobalite, SiO_2: symmetry analysis, domain structure and the dynamic nature of the β-phase. *Phys. Chem. Miner.*, **17**, 554–62.

Keen, D.A. (1997) Refining disordered structural models using reverse Monte Carlo methods: application to vitreous silica. *Phase Transitions*, **61**, 109–24.

Keen, D.A. (1998) Reverse Monte Carlo refinement of disordered silica phases. Pp. 101–19 in: *Local Structure from Diffraction* (S.J.L. Billinge and M.F. Thorpe, editors). Plenum, New York.

Keen, D.A. and McGreevy R.L. (1990) Structural modelling of glasses using reverse Monte Carlo simulation. *Nature*, **344**, 423–5.

Schmahl, W.W., Swainson, I.P., Dove, M.T. and Graeme-Barber, A. (1992) Landau free energy and order parameter behaviour of the α-β phase transition in cristobalite. *Zeits. Kristallogr.*, **201**, 125–45.

Wright, A.C. (1994) Neutron scattering from vitreous silica. V. The structure of vitreous silica: what have we learned from 60 years of diffraction studies? *J. Non-Cryst. Sol.*, **179**, 84–115.

Young, R.A. (1995) *The Rietveld Method*. International Union of Crystallography, Oxford University Press, Oxford, UK.

Zachariasen, W.H. (1932) The atomic arrangement in glass. *J. Amer. Chem. Soc.*, **54**, 3841–51.

[*Manuscript received 5 November 1999*]